PCCP

Accepted Manuscript

This is an *Accepted Manuscript*, which has been through the Royal Society of Chemistry peer review process and has been accepted for publication.

Accepted Manuscripts are published online shortly after acceptance, before technical editing, formatting and proof reading. Using this free service, authors can make their results available to the community, in citable form, before we publish the edited article. We will replace this *Accepted Manuscript* with the edited and formatted *Advance Article* as soon as it is available.

You can find more information about *Accepted Manuscripts* in the Information for Authors.

Please note that technical editing may introduce minor changes to the text and/or graphics, which may alter content. The journal's standard Terms & Conditions and the Ethical guidelines still apply. In no event shall the Royal Society of Chemistry be held responsible for any errors or omissions in this *Accepted Manuscript* or any consequences arising from the use of any information it contains.

ROYAL SOCIETY OF CHEMISTRY

www.rsc.org/pccp

Journal Name

RSCPublishing

ARTICLE

On the mechanism of methanol photooxidation to methylformate and carbon dioxide on TiO_2: An *operando*-FTIR study

Cite this: DOI: 10.1039/xoxxoooooox

Received ooth January 2012,
Accepted ooth January 2012

DOI: 10.1039/xoxxoooooox

www.rsc.org/

Mohamad El-Roz*, Philippe Bazin, Marco Daturi, Frederic Thibault-Starzyk

This work is a mechanistic study of total and partial methanol photooxidation using *operando* FTIR coupled to gas phase analysis techniques (gas-IR and MS). Methoxy and formate/formyl species play a key role in the reaction. Methoxy species are formed by thermal and photochemical dissociation of methanol. The formation of methylformate is favored by a high surface coverage by methoxy species. Surface and/or bridged oxygen atoms are also important actors. Steady State Isotopic Transient Kinetic Analysis (SSITKA) experiments showed that the limiting step is the conversion of chemisorbed formyl/formate and that methylformate is a secondary product from a reaction between methoxy and neighboring formyl species. Methanol concentration, among other reactions parameters, influences greatly the selectivity of photooxidation.

Introduction

Photocatalysis is an important and promising approach for green chemistry and energy sustainable solutions.[1-7] Titanium dioxide, for example is a photocatalyst used in very large-scale water purification applications[8], for hydrogen production from photocatalytic water splitting[9,10], and for selective photooxidation reactions in organic chemistry[11]. The photo-conversion of methanol is one a very interesting photocatalytic process[12]. Methanol represents a model for many organic compounds and is an appropriate molecular probe to explore oxide surface properties.[1,13-16] Methanol photochemistry on TiO_2 has often been the model for studying reaction mechanims. However, the roles of excited surface species (electrons, holes, and adsorbents) in surface chemistry on TiO_2 nanoparticles only start being understood. Panayotov et al. studied the role of oxygen in methanol photooxidation.[13] They showed that O_2, in promoting methanol photodecomposition, scavenges free electrons, and opens acceptor sites for the injection of new electrons during methoxy groups oxidation. They also proposed that O_2 increases the efficiency of methoxy groups oxidation, yet does not affect the hole-mediated oxidation mechanism that leads to final formate production. Zhou and co-workers[17] used scanning tunneling microscopy and two-photon photoemission to propose a two-step mechanism for the photooxidation of methanol to formaldehyde on TiO_2 (110). In their mechanism, the first step involves a photochemical O−H bond cleavage followed by a photochemical C−H bond cleavage. In another work, Shen and Henderson showed that the key step in methanol photochemistry on TiO_2 (110) is the thermal decomposition of methanol to methoxy groups, which is initiated by defects, coadsorbed oxygen adatom, or terminal OH groups, but not by bridging O sites.[18] Recently, the thermal decomposition of methanol was also studied by Philips and co-workers using mass spectrometry and scanning tunneling microscopy.[19] They concluded that coadsorbed oxygen atoms first interact thermally with CH_3OH to produce adsorbed CH_3O and H_2O. Then CH_3O species undergo a photo-oxidation reaction leading to the formation of CH_3OCHO species in a two-step process. In this case, CH_3O species are first converted to H_2CO then to HCO intermediates. A cross-coupling reaction involving CH_3O species allows then the formation of CH_3OCHO species. In this study, the preoxidation of the surface was considered to be essential to the initial formation of adsorbed CH_3O. The presence of HCO intermediates confirmed the hole-mediated dissociation of H_2CO by a bridge-bonded oxygen atom. Guo and co-workers proposed

Physical Chemistry Chemical Physics Accepted Manuscript

another mechanism for methanol photooxidation,[20] where the formation of CH_3OCHO does not involve a transient HCO intermediate. More recently Yuan and co-workers demonstrated that the photocatalytic dissociation of chemisorbed methanol to methoxy species occurs and contributes to the photocatalytic oxidation of methanol. Methylformate species are then formed from a photocatalytic cross coupling reaction of chemisorbed formaldehyde with chemisorbed methoxy groups on TiO_2 surface.[21] Various contradictory mechanisms were proposed recently for this reaction, showing there is no clear or generally accepted view of the reaction pathway. Thus, further investigations are required to better understand and elucidate the missing parts of the reaction mechanism, using spectroscopic tools to unravel surface adsorbed species and reaction intermediates.

In our previous works, we showed that methanol concentration has an important effect on the reaction selectivity.[1] This was attributed to the coverage level of TiO_2 surface by methanol. It was also related to other reaction parameters such as irradiation intensity, gas flow, temperature, etc….[1] In order to elucidate the mechanism of total and partial methanol photooxidations, *operando* FTIR spectroscopy coupled to gas phase analysis techniques (MS and gas-FTIR) is used in this work. *Operando* spectroscopy is a methodology wherein the spectroscopic characterization of materials undergoing reaction is coupled simultaneously with the measurement of catalytic activity and selectivity.[22] The primary concern of this methodology is to establish structure-reactivity/selectivity relationships of catalysts and thereby yield information about mechanisms. The *operando* approach can be applied to various reactor designs (perfectly stirred, plugflow, monoliths, etc,) with different kinetic behaviors (space velocity, contact time…). Different methanol concentrations and labeled methanol molecules $^{12}CH_3{}^{16}OH$, $^{12}CH_3{}^{18}OH$, $^{12}CD_3{}^{16}OH$ and $^{13}CH_3{}^{16}OH$ are also used. Coupling *operando* FTIR technique to steady state isotopic exchange kinetic analysis experiments reveals the mechanism of methylformate formation.

Results and Discussion

$^{12}CH_3{}^{16}OH$ photooxidation

We will first present the reaction behavior of methanol. Total conversion into CO_2 and H_2O is obtained during the photooxidation of 500 ppm of CH_3OH (Scheme 1-a) (T = 301 K; flow = 20 cm^3/min; □□= 365 nm; I_0 = 15 mW/cm^2). However, increasing the CH_3OH concentration to 1200 ppm promotes the production of methylformate as a methanol adduct under the same reaction conditions (Scheme 1). Such a result, in agreement with that observed in our previous work,[2] leads to investigate the influence of TiO_2 surface coverage by methanol on the selectivity of the reaction (CO_2 vs CH_3OCHO).

$$CH_3OH + 3/2O_2 \xrightarrow{TiO_2,\ h\nu} CO_2 + 3H_2O \quad (a)$$

$$2CH_3OH + O_2 \xrightarrow{TiO_2,\ h\nu} CH_3OCHO + 2H_2O \quad (b)$$

Scheme 1. The two possible reactions of methanol photooxidation.

In order to understand this effect and to highlight the total (Scheme 1-a) and partial (Scheme 1-b) methanol photooxidation mechanisms, the photooxidation of three additional methanol labeled molecules was performed: $^{12}CD_3{}^{16}OH$ (CD_3OH), $^{12}CH_3{}^{18}OH$ ($CH_3{}^{18}OH$) and $^{13}CH_3{}^{16}OH$ ($^{13}CH_3OH$).

CD_3OH photooxidation

In this part, CD_3OH was used to elucidate the first step of the reaction: dissociation of methanol on TiO_2. Then, we illustrate the role of TiOH groups in the photooxydation of surface methoxy, and in the condensation of physisorbed CD_3OH on TiOH site.

The photooxidation of CD_3OH on TiO_2 was performed with two different methanol concentrations: 500 ppm and 1200 ppm. Figure 1 shows the evolution, during this reaction, of the MS signals of methanol (m/z = 31), carbon dioxide (m/z = 44), water (m/z = 18; 19; 20), and methyl formate (m/z = 64), in addition to the relative infrared intensities of methoxy groups (1108 cm^{-1}) and formate species (1568 cm^{-1}) adsorbed on TiO_2 surface. With 500 ppm of methanol, CD_3OH photooxidation produces three types of water molecules: H_2O, HOD and D_2O (Figure 1-C) with a total conversion of methanol into CO_2 (Figure S-2). A quantitative discussion of the D_2O, HOD and H_2O ratios cannot be achieved for the easy O-H/O-D isotopic exchange between species in the gas phase (D_2O/H_2O; D_2O/CD_3OH) even at low temperature. Consequently, the results are discussed only qualitatively:

- A high amount of H_2O is produced in the first five minutes of irradiation. It might result from an oxidation of two neighboring d_3-methanol molecules (one H atom/molecule) and/or from a condensation of CD_3OH with TiOH sites.
- In a second time (> 5 min), H_2O decreases very rapidly and a higher amount of HOD and heavy water (D_2O) is produced.
- The water MS signals become stable after 30 minutes of irradiation and a very low H_2O yield is detected in the gas flow.

This suggests that when methanol is adsorbed on the surface in large amounts, at the beginning of the reaction, it is thermally dissociated and leads to the formation of surface methoxy groups and large amounts of TiOH groups on the surface of TiO_2 (Figures 1-E and S3). In a further photochemical step, TiOH sites and physisorbed CD_3OH condensate to form some more surface methoxy groups and non-labeled water molecules.

Further on during the reaction, the amount of adsorbed methanol decreases, and surface TiOH groups are progressively exchanged and deuterated by labeled molecules in the reaction medium (D_2O molecules from $CD_3O_{(a)}$ photooxydation). The intensity of the IR bands for TiOH (3700-3000 cm^{-1}) progressively decrease, replaced by TiOD vibration bands at 2700-2400 cm^{-1} (Figure 2). The H/D isotopic exchange between D_2O/TiOH, and D_2O/H_2O, produced in relatively high amount in the first minutes of irradiation, led to an increase of DOH concentration in the gas phase. This explains the kinetic behaviors of D_2O (slow increase) and HOD (increase followed by a slow decline) in the gas flow.

Physical Chemistry Chemical Physics Accepted Manuscript

This journal is © The Royal Society of Chemistry 2012

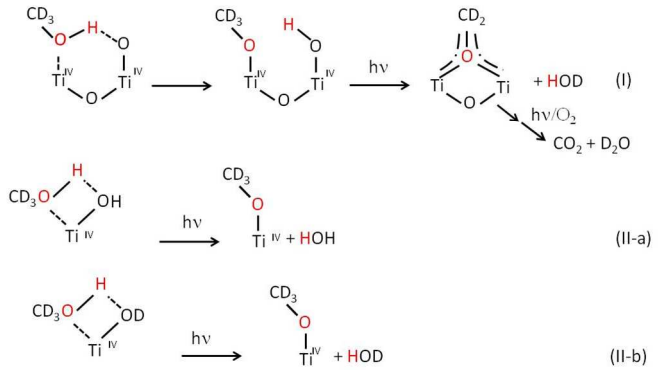

Scheme 2. Mechanism of formation of methoxy species and water molecules during CD_3OH photooxidation. Doted lines (---) correspond to a physisorption and/or chemisorption (dissociative adsorption) of methanol-d3 on the TiO_2 surface sites. The partially doted lines (–·–) correspond to an electron delocalization between the TiO_2 surface sites and adsorbed species/intermediates).

At higher methanol concentration (1200 ppm), the proportion of unlabeled water increases considerably in the gas flow (Figure 1-C, mechanism in scheme 2, II-a). In parallel, an increase in the methoxy groups adsorbed on the surface is observed (Figure 1-E). The selectivity of the reaction is also changed; in addition to CO_2, a totally deuterated methylformate is produced (Figure 1-D), (60% CO_2-selectivity with 75% methanol conversion (Figure S-2)). This aspect is discussed later in this paper using $CH_3{}^{18}OH$ and $CH_3OH/{}^{13}CH_3OH$ SSITKA experiments.

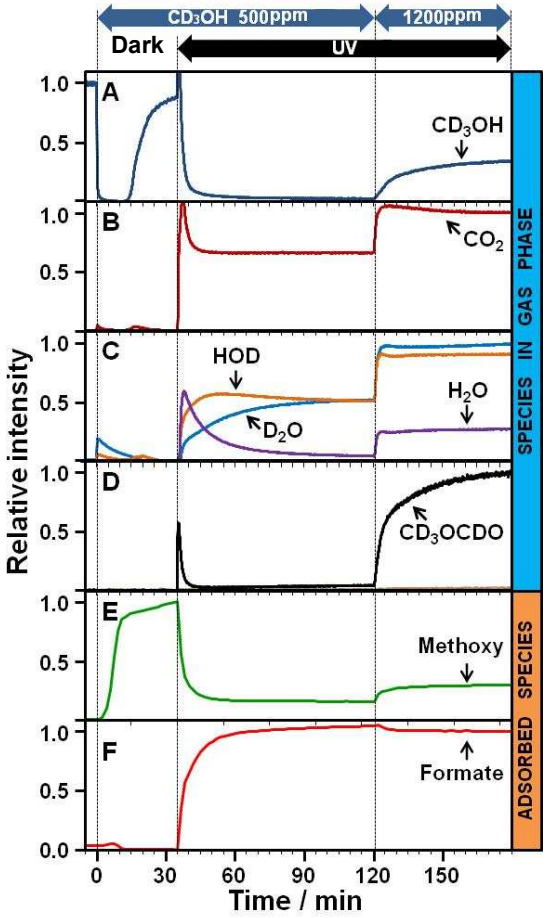

Figure 1. Evolution of gas phase products (A-D) and adsorbed species on TiO_2 (E-F) before and during the photooxidation of 500 and 1200 ppm of CD_3OH. t = 0 min is the time where the Ar flow saturated with 500 ppm of methanol was sent to the reactor. At t = 35 min, the UV lamp is turned-on. At t = 120 min, methanol concentration was increased from 500 ppm to 1200 ppm. (reaction conditions: T = 301 K; flow = 20 cm^3/min; λ = 365 nm; I_0 = 15 mW/cm^2).

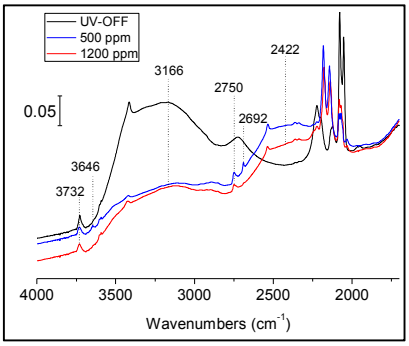

Figure 2. IR spectra of TiO_2 surface during CD_3OH photooxidation before and after irradiation, under 500 ppm and 1200 ppm CD_3OH, respectively. This figure shows an isotopic exchange between TiOH groups (3800-2700 cm^{-1}) and HOD/D_2O and the formation of TiOD groups (2750-2400 cm^{-1}). A higher intensity of the hydrogen bonded TiOH vibration band at 3166 cm^{-1} could be observed after increasing the methanol concentration, with the formation of a new isolated TiOH/TiOD sites with a vibration band at 3646/2692 cm^{-1}.

Physical Chemistry Chemical Physics Accepted Manuscript

$CH_3{}^{18}OH$ photooxidation

The role of oxygen (bridged, molecular and/or adatom) in methanol photooxidation was studied in the photooxidation of labeled ^{18}O-methanol ($CH_3{}^{18}OH$) in the presence of an excess of $^{16}O_2$. This study also helps highlighting the mechanism of methyl formate formation. Figure 3 shows the evolution of the relative intensities of characteristic MS signals of gas phase species (A-D) and those of the characteristic IR bands of adsorbed surface species (E-F) during $CH_3{}^{18}OH$ photooxidation. At low methanol concentration (500 ppm), the photooxidation is almost complete and provides all possible CO_2 isotopes: $C^{16}O_2$, $C^{16}O^{18}O$, and low $C^{18}O_2$ amounts (Figure 3-B). Most of the water produced is unlabeled, with about 20% of $H_2{}^{18}O$ (Figure 3-C).

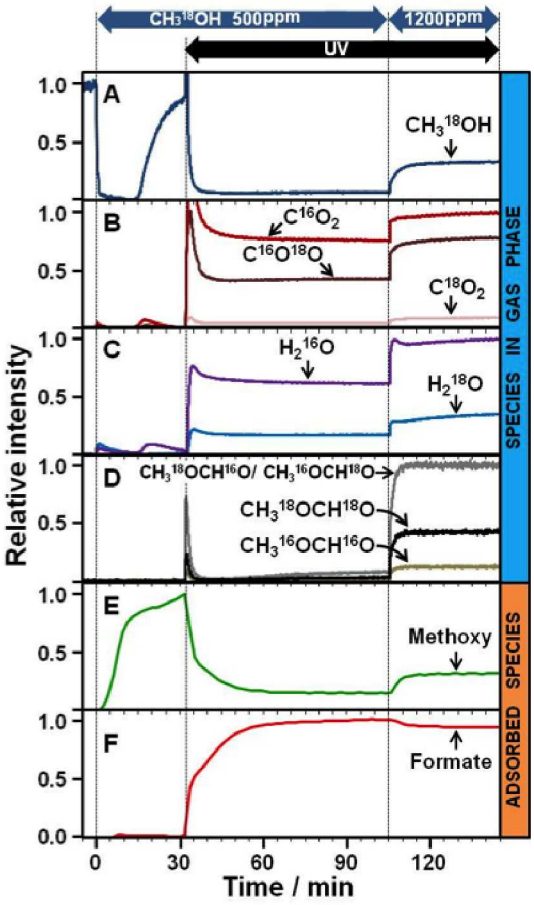

Figure 3. Evolution of the gas phase products (A-D) and adsorbed species on TiO_2 (E-F), before and during the photooxidation of 500 and 1200 ppm of $CH_3{}^{18}OH$. t = 0 min is the time when the Ar flow saturated with 500 ppm of methanol was sent to the reactor. At t = 32 min, the UV lamp was turned-on. At t = 105 min, the methanol concentration was increased from 500 ppm to 1200 ppm. (T = 301 K; flow = 20 cm^3/min; λ = 365 nm; I_0 = 15 mW/cm^2).

At higher concentration (1200 ppm $CH_3{}^{18}OH$), similar results are obtained, with a slight increase in the relative amount of labeled species (Table 2). The labeled and unlabeled methylformates are formed in various proportions:

1) $CH_3{}^{18}OCH^{16}O$ (1-a) + $CH_3{}^{16}OCH^{18}O$ (1-b) = 64±5 %

2) $CH_3{}^{18}OCH^{18}O$ = 29±5 %

3) $CH_3{}^{16}OCH^{16}O$ = 8±5 %

Methylformates labeled with one oxygen atom (1), both having the same mass signal of m/z = 62, represent two thirds of the total methylformates produced. Comparing IR spectra of unlabeled and ^{18}O-labeled methanol photooxidation experiments (under similar conditions) shows that in the labeled experiment, the C-^{16}O-C vibration band (1209 cm^{-1}) almost totally disappears, while the C=^{16}O (carbonyl groups) band (1770 cm^{-1}) only decreases less than 15% (these wavenumbers were used to minimise the overlapping of the labeled functions vibration bands). Formates are thus mostly labeled on the methoxy group ($CH_3{}^{18}OCH^{16}O$), and not on the carbonyl group. The unlabeled carbonyl function (<20 %) actually corresponds to methylformate with two ^{16}O atoms (8±5%), which could originate in the imperfect labeling of methanol used (95% ^{18}O). The reaction of $CH_3{}^{18}OH$ leads to approximately half the amount of $C^{16}O_2$ formed from $CH_3{}^{16}OH$ (Figure S-3), in agreement with measurements presented in Table 2 (56±5% for $C^{16}O_2$).

The high yield of unlabeled oxygen atoms in the products of ^{18}O-methanol photooxidation (water, carbon dioxide and methylformate) shows the important contribution of oxygen molecules, oxygen adatoms (formed form the dissociation of O_2 on oxygen vacancy sites) and/or of bridged oxygen on TiO_2 surface in methanol photooxidation. These unlabeled oxygen atoms are introduced during the formation of formyl/formate intermediates, while the methoxy groups are not dissociated (see also Figure S-4).

These results suggest the formation of methylformates from a cross coupling reaction between methoxy groups and chemisorbed $HC^{16}O$ (formyl) transient species, rather than with chemisorbed formaldehyde species (hypothesis of Yan et al. [21]). In the last case, only $CH_3{}^{18}OCH^{18}O$ would have been obtained (the oxygen of methanol still being attached to its initial carbon atom).

Physical Chemistry Chemical Physics Accepted Manuscript

This journal is © The Royal Society of Chemistry 2012

Table 2. Relative yield of natural and labeled molecules in final products obtained from the photooxidation of ^{18}O-methanol (methanol concentrations = 500 and 1200 ppm). The errors are estimated to less than 5% by reproducing the experiment three times.

	$CH_3{}^{18}OH$ / ppm	
Assignment	500	1200
Water		
$H_2{}^{16}O$	0.79	0.74
$H_2{}^{18}O$		0.21
Carbon dioxide		
$C^{16}O_2$	0.61	0.56
$C^{16}O\,{}^{18}O$	0.36	0.41
$C^{18}O_2$	0.03	0.03
Methyl formate		
$CH_3{}^{16}OCH^{16}O$	0.00	0.08
$CH_3{}^{18}OCH^{16}O$	0.00	0.64
$CH_3{}^{18}OCH^{18}O$	0.00	0.29
Methoxy		
$CH_3{}^{16}O$	< 0.10	< 0.10
$CH_3{}^{18}O$	>0.90	>0.90
Formate		
$HC^{16}O^{16}O$	0.65	0.65
$HC^{18}O^{16}O$	0.35	0.35

Steady State Isotopic Transient kinetic analysis (SSITKA): CD_3OH/CH_3OH, $CH_3{}^{16}OH/CH_3{}^{18}OH$ and $^{12}CH_3OH/^{13}CH_3OH$:

SSITKA is a methodology for obtaining transient conditions while remaining under the required chemical and/or kinetic steady state environment for a given reaction. It has already been used for a better understanding or for clarifying the mechanism of a catalytic reaction, and sometimes to determine the activation energy.[23-26] We employed it recently to obtain information about the kinetics of methanol photooxidation reaction.[2]

Here, Steady State Isotopic Transient (SSIT) studies of labeled and unlabeled methanol were performed. Transient MS signals at m/z = 61 and m/z = 63 were observed when switching from CD_3OH to CH_3OH (Figure S-5). These signals are assigned to the formation of CH_3OCDO and CD_3OCHO, respectively. The transient MS signal at m/z = 61 observed upon the isotopic exchange from CH_3OH to $^{13}CH_3OH$ is assigned to the formation of two labeled methylformates: $CH_3O^{13}CHO$ and $^{13}CH_3OCHO$, respectively. These results demonstrate, without any doubt, that methyl formate species are formed from a cross coupling reaction between methoxy group and formyl/formate species.

In the CD_3OH/CH_3OH steady state isotopic transient experiment, the disappearance of CD_3OCHO was two times faster than that of CH_3OCDO (Figure S-6). This demonstrates that the chemisorbed methoxy species on the TiO_2 surface are more reactive than formyl/formate species. Therefore, formyl/formate conversion is the limiting step in the methanol photooxidation reaction.

Monitoring the surface species by FTIR provided additional information to SSITKA. After UV irradiation, new bands assigned to mono and bidentate formate species adsorbed on the catalyst surface appeared (Figure S-7; Table 1). Due to less overlap between the IR vibration bands of surface species formed during the photooxidation of CH_3OH and $^{13}CH_3OH$ (Figure 4), the $CH_3OH/^{13}CH_3OH$ SSITKA experiment is easier to interpret and will be discussed here in detail.

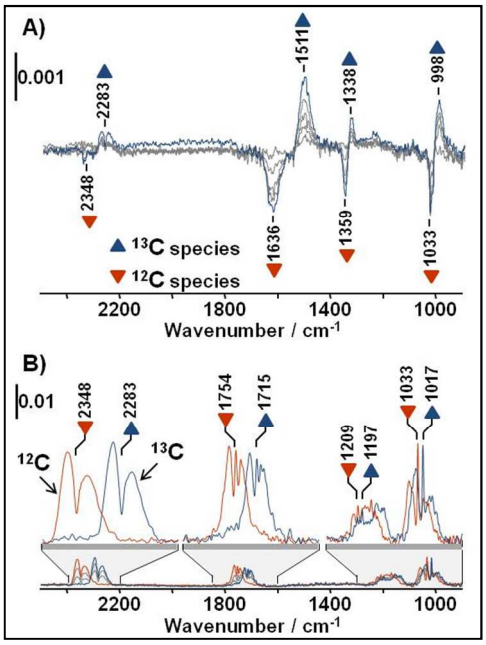

Figure 4. Evolution of IR spectra versus time during photooxidation of 1200 ppm of methanol at 301 K in synthetic air during $^{12}CH_3OH/^{13}CH_3OH$ SSITKA experiment: A) adsorbed species on TiO_2-P25 (supported-TiO_2 powder; 5.4 s/spectrum)) and B) species in gas phase. (flow = 20 cm^3/min; 301 K; $I_{0(366)}$~15 mW/cm^2; □ = 366 nm; I_0 = 15 mW/cm^2).

The kinetics of the formate exchange on the surface was discussed in our previous work.[2] It was different from that of the gas phase products. This difference may be derived from:

1) The existence of different active sites on TiO_2 surface; less active sites that are easily detected, and very active but less visible sites.

and/or

2) The shading effect: activity difference depending on whether the sites are near to the wafer surface or not (inhomogeneous irradiation with the depth of the catalyst in the catalyst bed).[22]

Series of experiments were therefore performed to test these hypotheses by varying the thickness of the pellets or the amount of the catalyst: i) A self-supporting wafer 20 mg (diameter 16 mm, thickness 50-70 μm), ii) 5 mg pellet supported by a stainless steel grid (diameter 6 mm, thickness 50-70 μm), and iii) TiO_2 powder deposited on a KBr window (diameter 16 mm; <10 μm of thickness). A significant difference was observed between the three cases, confirming the shading effect (Figure S-8). In the case of the TiO_2 powder supported on KBr pellet, the shading effect was at its minimum. The kinetics were then similar throughout the catalyst and we used this case for the comparison of different kinetics during exchanges.

Physical Chemistry Chemical Physics Accepted Manuscript

In the $^{12}CH_3OH/^{13}CH_3OH$ transient experiment, the evolution of surface formate species parallels that of CO_2 produced (Figure 5): formates are intermediates to the formation of CO_2.

The m/z = 61 signal is due to $^{12/13}CH_3O^{13/12}CHO$ methylformates produced from the methoxy/formate cross coupling reaction. The non-Gaussian form of the kinetic of this transient signal points to a difference in the kinetics of methoxy and formate groups on the surface. ^{12}C-methoxy disappear rapidly and are quickly replaced by ^{13}C-methoxy groups, while ^{12}C-formate remain longer on the surface after exchange, and the formation of $^{12}CH_3O^{13}CHO$ is faster than that of $^{13}CH_3O^{12}CHO$ (Figure 5-C-(d). This show that formate and methoxy are the main intermediates of methylformate.

CO_2 is produced from the oxidation of formates, and the conversion of surface formates is the limiting step of the photooxidation of methanol.

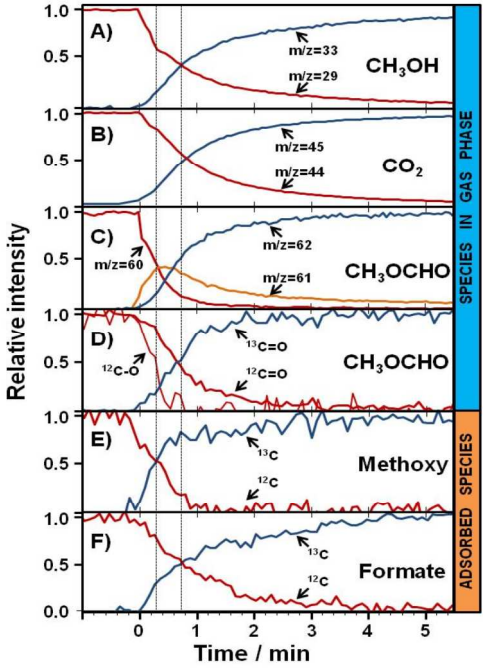

Figure 5. Evolution of adsorbed species on TiO_2 surface and in gas phase during methanol photooxidation versus time of the $^{12}CH_3OH/^{13}CH_3OH$ SSITKA experiment (t = 0 min correspond to the $^{13}CH_3OH/CH_3OH$ exchange). TiO_2 powders were deposited on a KBr window (m_{TiO2} ≈3 mg; diameter = 16 mm; <10 μm of thickness; methanol concentration = 500 ppm; T = 301 K; flow = 20 cm^3/min; λ = 365 nm; I_0 = 15 mW/cm^2).

Scheme 3 summarizes these results, taking into account the experimental ratios between products obtained in $CH_3{}^{18}OH$ photooxidation. It shows the successive steps in the photooxidation of a molecule of labeled methanol, and the various possible cases.

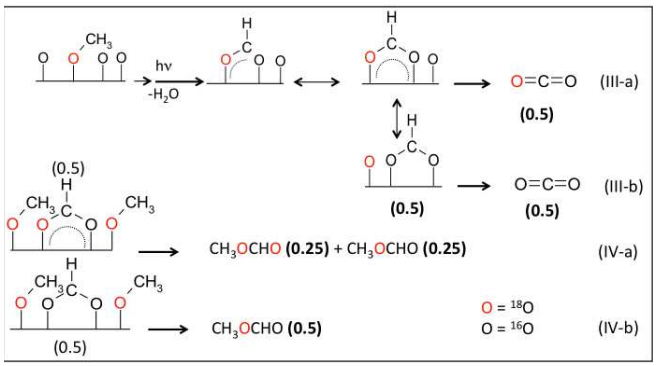

Scheme 3. Mechanism of the formation of carbon dioxide and methylformate during $CH_3{}^{18}OH$ photooxidation. ^{16}O (in black) correspond to the oxygen coming from TiO_2 surface (bridged oxygen) and/or molecular oxygen chemisorbed on TiO_2 (oxygen adatom), while ^{18}O (in red) is coming from $CH_3{}^{18}OH$.

The statistical values of the different labeled CO_2 yields, as shown in Scheme 3, are rather different from those obtained experimentally (Table 2). Thus, $C^{18}O^{18}O$ is not expected theoretically, but was detected in small amounts (3%). It can be obtained only via labeled formate ($^{18}OCHO^{18}$), which is not expected here but can nevertheless be formed via ^{18}O-formyl intermediates bridged over ^{18}O-surface sites. Therefore, this oxygen is probably inserted in the surface from the scrambling of formate species on the preoxidized TiO_2 surface. The expected statistical value of ^{18}O-methyl formate formation is 75% (or 70% if we take into account the $CH_3{}^{16}OH$ impurity present in $CH_3{}^{18}OH$ used initially). Only 64% was experimentally measured, which might also be assigned to the already mentioned scrambling of formates on the preoxidized TiO_2 surface.

As shown in Scheme 2, formyl species (HCO) are also intermediates in the reaction and a CHO/OCHO equilibrium exists on the surface. Adsorption of pure methylformate on a clean TiO_2 surface also led to spectral features of surface formates and surface methoxy groups, evidencing a reversible dissociation of methylformates in possible equilibrium with methoxy groups and formates .

Conclusions

A global mechanism can be proposed for methanol photooxidation in Scheme 4. The main pathway for methanol photooxidation goes through the chemisorption of methanol as surface methoxy species, then their oxidation into formates and, finally, into CO_2. In parallel, neighboring adsorbed formates and methoxy groups can give rise to methylformates, as secondary species. This also explains the relationship between the coverage of TiO_2 by methoxy groups (depending on methanol concentration) and methylformate produced as secondary product: increasing the methanol/methoxy concentration promotes methoxy and formyl cross coupling reaction versus formate oxidation, which is the slow step in the main reaction. These mechanistic evidences bring information on the real reaction dynamics of methanol photooxidation on titania, discriminating between reaction intermediates and spectator or byproduct species. Moreover, they highlight the effects of the thermodynamic parameters (temperature, contact time, concentration, etc.)[1] on the selectivity of methanol photooxidation. These findings open the way to determining the apparent rate

Physical Chemistry Chemical Physics Accepted Manuscript

This journal is © The Royal Society of Chemistry 2012

constants of the different reaction pathways of methanol photooxidation.

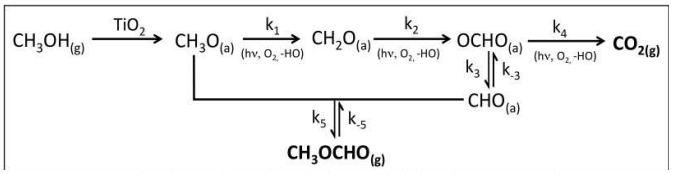

Scheme 4. Mechanism of methanol photooxidation into CO_2 and CH_3OCHO. The k_i parameters represent the apparent kinetic constants of each reaction step, to be determined in an incoming work.

Experimental Section

The photocatalytic oxidation of methanol was performed using a new *operando* IR reactor described elsewhere.[1] TiO_2-P25 (Evonik-Degussa) was pressed into self-supported wafers (Ø = 16 mm, m = 10 mg/cm^2; thickness = 50-60 µm (measured by Micromaster-IP54)) or laid as supported-TiO_2 powder (<10 µm) on a KBr window (for a SSITKA experiment). The IR reactor-cell was connected to gas lines with gas mixing devices and mass flow controllers. Two gas mixtures can be prepared and sent independently to the reactor cell. Exhaust gases (reactants and/or reaction products) can be analyzed by a Quadrupole Mass Spectrometer (Pfeiffer Omnistar GSD 301), while complementary information on the gas phase can be gained by IR spectroscopy with a gas micro-cell. IR spectra (64 scans per spectrum) of the catalyst under working conditions were collected at a time resolution of 1 spectrum each 2 minutes with a Thermo Scientific Nicolet 6700 spectrometer, equipped with a MCT detector. A greater temporal resolution has been used for SSITKA experiments: 10 scans per spectrum and 1 spectrum collected each 5.4 seconds. All IR spectra are displayed as absorbance. For this specific study, the system was equipped with four saturators in the same thermostatic bath in order to obtain similar temperatures. A fixed concentration of vaporized methanol, either in its natural form, 99.0% $^{13}CH_3OH$ enriched (Cambridge Isotope Laboratories), 99.8% CD_3OH (from Aldrich) or 95.0% $CH_3{}^{18}OH$ (Aldrich) is sent, via a four ways valve, under the flow conditions: 500 or 1200 ppm methanol, 20% oxygen in Argon. Therefore, gas hourly space velocities (GHSV) are equal to 60 000 h^{-1} and 360 000 h^{-1} for self-supported wafers and supported-TiO_2 powder on KBr, respectively. According to recent results, the conditions used in this work ensure reliable and representative results of a real process.[27,28] The transmission IR reactor-cell used in this study is able to generate relevant data for a correct kinetic interpretation of the reaction. To calculate the methanol conversion, a calibration curve was drawn to establish the linear relationship between the concentration of methanol and the MS signal intensity or IR band intensity (at m/z = 29 and 1038-1026 cm^{-1} respectively), for $^{12}CH_3{}^{16}OH$ (Figure S-1). The reaction was studied at 301 K. The irradiation was applied with a Xe-Hg lamp (LC8 Spot Light Hamamatsu, L10852, 200 W) and UV-light guide (A10014-50-0110) mounted at the entrance of the *operando* IR cell.[1] A monochromatic 365 nm band pass filter was used ($I_{0(365nm)}$~15 mW/cm^2). The photocatalyst samples were activated at 473 K (5 K/min) for 1h under synthetic air and polychromatic UV irradiation and then cooled down to 301 K (5 K/min) before each experiment. The characteristic IR bands used to quantify the gas phase and adsorbed species before and during natural and labeled methanol photooxidation reactions by FTIR are reported in Table 1.

Table 1. Table 1. Infrared bands absorption (cm^{-1}) and assignment of relevant species observed in the gas phase and adsorbed on TiO_2 after exposition to various labeled methanol and UV light.

	Band frequency / cm^{-1}			
Assignment	$^{12}CH_3{}^{16}OH$	$^{13}CH_3{}^{16}OH$	$^{12}CH_3{}^{18}OH$	$^{12}CD_3{}^{16}OH$
Methanol$_{(gas)}$				
□ν□(OC)	1033 [a,b]	1017 [b]	1007 [i]	984 [a]
Carbon dioxide$_{(gas)}$				
□ν□ (CO_2)	2349 [c]	2283 [d]	2332 [c,e]	2349 [c]
Methylformate$_{(gas)}$				
□ν (C-O)	1209 [f,g]	1197 [g]	1190 [i]	1201 [f]
□ν (C=O)	1754 [f,g]	1715 [g]	1719 [i]	1745 [f]
Methanol$_{(ads.)}$ [h]				
□ν (OC)	1023 [i]	1001 [i]	993 [i]	979 [i]
Methoxy$_{(ads.)}$ [h]				
□ν (OC) linear	1110 [i]	1088 [i]	1083 [i]	
□δ□(CD_3)				1108 [i]
Formate$_{(ads.)}$				
ν_{as}(COO)	1571 [g]	1528 [g]	1532 [j,k]	1568 [i]
□ν_s(COO)	1362 [g]	1342 [g]	1335 [j]	1336 [i]
δ	1378 [g]	1378 [g]	1374 [j]	1023 [i]

[a] According to reference [29]. **[b]** According to reference [30]. **[c]** According to reference [31]. **[d]** According to reference [32]. **[e]** ν□($C^{16}O^{18}O$) frequency. The ν□($C^{18}O_2$) band intensity at 2314 cm^{-1} [31] is very weak in our work. **[f]** According to reference [33]. **[g]** According to reference [2,34]. **[h]** Frequency of residual methanol/methoxy groups bands under UV. The present of different bands of methoxy in the C-O vibration regions is probably due to presence of methoxy species (linear, type I, type II, etc.). These species have been shown a relatively similar kinetic behavior during SSITKA experiments. **[i]** This work. **[j]** According to reference [35].**[k]** Frequency of□□ ν_{as}(COO) is pointed at 1563 cm^{-1} but this band is due to the mixture of $HC^{16}O^{18}O$ (35%) and $HC^{16}O^{16}O$ (65%) adsorbed species. By subtraction of□□ ν_{as} ($C^{16}O^{16}O$) contribution, the ν_{as}($C^{16}O^{18}O$) is finally pointed at 1532 cm^{-1}.

The characteristic MS signals used to follow the evolution of the species in gas phase are: $^{12}CH_3OH$ (m/z=33); $^{12}CO_2$ (m/z=44); $^{12}CH_3O^{12}CHO$ (m/z=60); $^{13}CH_3OH$ (m/z=29); $^{13}CO_2$ (m/z=45); $^{13}CH_3O^{12}CHO$; $^{12}CH_3O^{13}CHO$ (m/z=61); $^{13}CH_3O^{13}CHO$ (m/z=62); $CH_3{}^{18}OH$ (m/z=31); $C^{16}O_2$ (m/z=44); $C^{18}O^{16}O$ (m/z=46) ; $C^{18}O_2$ (m/z=48) ; $H_2{}^{16}O$ (m/z=18) ; $H_2{}^{18}O$ (m/z=20) ; $CH_3{}^{16}OCH^{16}O$ (m/z=60) ; $CH_3{}^{16}OCH^{18}O/CH_3{}^{18}OCH^{16}O$ (m/z=62) ; $CH_3{}^{18}OCH^{18}O$ (m/z=64); CD_3OH (m/z=35); DOH (m/z=19); D_2O (m/z=20)); CH_3OCDO (m/z=63); CD_3OCHO (m/z=61) and CD_3OCDO (m/z=64). IR bands used to calculate the evolution of the TiO_2 adsorbed species are: $CH_3{}^{18}O$ (methoxy) (area of the characteristic vibration bands at 1033, 998

Physical Chemistry Chemical Physics Accepted Manuscript

1083 and 1108 cm^{-1} for labeled $^{12}CH_3OH$, $^{13}CH_3OH$, $CH_3{}^{18}OH$ and CD_3OH, respectively); HCOO (formate) (area of the characteristic vibration bands at 1571 cm^{-1}, 1528, 1532 and 1568 cm^{-1} for labeled ^{12}C, ^{13}C, ^{16}O and DCOO respectively).

Acknowledgements

M. El-Roz and F. Thibault-Starzyk acknowledge the European Regional Development Fund Franco-British INTERREG IVA (Project E3C3, Ref. 4274) for financial support.

Notes and references

[a] Laboratoire Catalyse et Spectrochimie, ENSICAEN, Université de Caen, CNRS, 6, boulevard du Maréchal juin, 14050 Caen, France.

Electronic Supplementary Information (ESI) available: Calibration curves of methanol and CO_2, MS signals and IR spectra of the gas phase of natural and labeled methanol photooxidation. See DOI: 10.1039/b000000x/

[1] M. El-Roz, M. Kus, P. Cool, F. Thibault-Starzyk, *J. Phys. Chem. C* 2012, **116**, 13252.
[2] M. El-Roz, P. Bazin, M. Daturi, F. Thibault-Starzyk, *ACS Catal.* 2013, **3**, 2790.
[3] M. El-Roz, Z. Haidar, L. Lakiss, J. Toufaily, F. Thibault-Starzyk, *RCS Advances* 2013, **3,** 3438.
[4] M. El-Roz, L. Lakiss, J. El-Fallah, O. I. Lebedev, F. Thibault-Starzyk, V. Valtchev, *Phys. Chem. Chem. Phys.* 2013, **15**, 16198.
[5] H. Chen, C. E. Nanayakkara, V. H. Grassian, *Chem. Rev.* 2012, **112**, 5919.
[6] T. P. Yoon, *ACS catal.* 2013, **3**, 895.
[7] M. d. O. Melo, L. A. Silva, *J. Photochem. Photobio. A.: Chem.* 2011, **226**, 36.
[8] K. Hashimoto, H. Irie, A. Fujishima, *Jpn. J. Appl. Phys.* 2005, **44**, 8269.
[9] J. S. Jang, S. H. Choi, H. G. Kim, J. S. Lee, *J. Phys. Chem. C* 2008, **112**, 17200.
[10] E. Reisner, D. J. Powell, C. Cavazza, J. C. Fontecilla-Camps, F. Armstrong, A. *J. Am. Chem. Soc.* 2009, **131**, 18457.
[11] D. Tsukamoto, Y. Shiraishi, Y. Sugano, S. Ichikawa, S. Tanaka, T. Hirai, *J. Am. Chem. Soc.* 2012, **134**, 6309.
[12] M. Pelaez, N. T. Nolan, S.C. Pillai, M. K. Seery, P. Falaras, A. G. Kontos, P. S.M. Dunlop, J. W.J. Hamilton, J.A. Byrne, K. O'Shea, M. H. Entezari, D. D. Dionysiou, *Appl. Catal. B: Env.* 2012, **125**, 331.
[13] D. Panayatov, P. A. DeSario, J. J. Pietron, T. H. Brintlinger, L. C. Szymczak, D. R. Rolison, J. R. Morris, *J. Phys. Chem. C* 2013, **117**, 15035-15049.
[14] K. Kähler, M. C. Holz, M. Rohe, A. C. V. Veen, M. Muhler, *J. Catal.* 2013, **299**, 162.
[15] L. J. Burcham, L. E. Briand, I. E. Wachs, *Langmuir* 2001, **17**, 6175.
[16] C. Binet, M. Daturi, *Catal. Today* 2001, **70**, 155.
[17] C. Y. Zhou, Z. B. Ma, Z. F. Ren, X. C. Mao, D. X. Dai, X. M. Yang, *Chem. Sci.* 2011, **2**, 1980.
[18] M. Shen, M. Henderson. *J. Phys. Chem. C* 2012, **116**, 18788.
[19] K. R. Phillips, S. C. Jensen, M. Baron, S.-C. Li, C. M. Friend, *J. Am. Chem. Soc.* 2013, **135**, 574.
[20] Q. Guo, C. Xu, W. Yang, Z. Ren, Z. Ma, D. Dai, T. K. Minton, X. Yang, *J. Phys. Chem. C* 2013, **117**, 5293.
[21] Q. Yuan, Z. Wu, Y. Jin, L. Xu, F. Xiong, Y. Ma, W. Huang, *J. Am. Chem. Soc.* 2013, **135**, 5212.
[22] Miguel A. Bañares, *Catal. Today*, 2005, **100**, 71.
[23] P. Bazin, S. Thomas, O. Marie, M. Daturi, *Catal. Today,* 2012, **182**, 3.
[24] A.M. Efstathiou, X.E. Verykios, *Appl. Catal. A: Gen.* 1997, **151**, 109.
[25] G.G. Olympiou, C.M. Kalamaras, C.D. Zeinalipour-Yazdi, A.M. Efstathiou, *Catal. Today*, 2007, **127**, 304.
[26] J. Wang, V. F. Kispersky, W. N. Delgass, F. H. Ribeiro, *J. Catal.* 2012, 289, 171.
[27] S. B. Rasmussen, S. Perez-Ferreras , M. A. Bañares , P. Bazin , M. Daturi *ACS Catalysis*, 2013, **3**, 86.
[28] S. Rousseau, O. Marie, P. Bazin, M. Daturi, S. Verdier, V. Harle, *J. Am. Chem. Soc.* 2010, **132**, 10832.
[29] M. F. Whalley, *J. Chem. Phys.*, 1961, **34**, 1554.
[30] R.B. Bernstein, J.E. Lambert, F.F. Cleveland, *J. Chem. Phys.*, 1953, **10**, 1903.
[31] T. Konno, S. Yamaguchi, Y. Oza, *J. Molecular Spectroscopy*, 2011, **270**, 66.
[32] N. Bion, J. Saussey, C. Hedouin, T. Seguelong, M. Daturi, *Phys. Chem. Chem. Phys.*, 2001, **3**, 4811.
[33] H. Susi and T. Zell, *Spectrochim. Acta*, 1963, **19**, 1933.
[34] M. El-Roz, P. Bazin, F. Thibault-Starzyk, *Catal. Today* 2013, **205**, 111.
[35] L.-F. Liao, C.-F. Lien, D.-L. Shieh, M.-T. Chen, and J.-L. Lin, *J. Phys. Chem. B,* 2002, 106, 11240.

Physical Chemistry Chemical Physics Accepted Manuscript

 This journal is © The Royal Society of Chemistry 2012